Title

Archaeomagnetic Dating of Pyrotechnological Contexts: a Case Study for Copper Smelting Sites in the Central Timna Valley, Israel

Journal

Archaeometry, 60(3)

ISSN

0003-813X

Authors

Peters, I
Tauxe, L
Ben-Yosef, E

Publication Date

2018-06-01

DOI

10.1111/arcm.12322

Peer reviewed

archaeometry

Archaeometry ••, •• (2017) ••–•• doi: 10.1111/arcm.12322

ARCHAEOMAGNETIC DATING OF PYROTECHNOLOGICAL CONTEXTS: A CASE STUDY FOR COPPER SMELTING SITES IN THE CENTRAL TIMNA VALLEY, ISRAEL*

I. PETERS,[1] L. TAUXE[2] and E. BEN-YOSEF[1]†

[1]*Department of Archaeology and Ancient Near East Cultures, Tel Aviv University, Tel Aviv 6997801, Israel*
[2]*Scripps Institution of Oceanography, University of California, San Diego, La Jolla, CA 92037, USA*

This study is focused on establishing age constraints for several copper slag deposits at the centre of the Timna Valley (Israel) via reconstruction of their ancient geomagnetic intensities as recorded by the individual slag samples at the time of their formation. The results show a correlation between the location of the slag deposits (labelled as individual 'mounds' in our survey) and their inferred ages, reflecting varying socio-economic and political dynamics in the region. While the slag mounds found at the unprotected foothills represent a variety of dates (mostly Early Islamic), the slag mounds on the hilltops are chronologically constrained to the early Iron Age (late 11th to 10th centuries BCE), supporting the idea for a need for protection during this period. Furthermore, in comparing the new data with previous archaeomagnetic studies from Timna, we can assert the existence of simultaneous copper production at the archaeological Sites 30, 30a and 34. This gives further support to the claim of intense smelting in the central Timna Valley during the early Iron Age. Finally, this project demonstrates the potential of archaeomagnetic experiments to provide chronological insights, and their particular advantage in addressing pyrotechnology-related cases.

KEYWORDS: ARCHAEOMAGNETISM, ARCHAEOMETALLURGY, COPPER SLAG, IRON AGE, TIMNA, ARABAH VALLEY, COPPER SMELTING

INTRODUCTION

Located in southern Israel, the Timna Valley (Fig. 1) is host to over 200 archaeological sites, the *raison d'être* for which was copper production (e.g., Rothenberg and Glass 1992). However, despite decades of research (Glueck 1935; Conrad and Rothenberg 1980; Rothenberg 1999a, b), the timing of the main smelting sites is still debated: while in the 1930s these sites were dated to the Iron Age (10th century BCE) and considered to be the source of King Solomon's riches (Glueck 1935), at the end of the 1960s they were redated to the Late Bronze Age (13th to mid-12th centuries BCE; Rothenberg 1999b), only to be redated once again to the early Iron Age (late 12th to ninth centuries BCE; Ben-Yosef *et al.* 2012). The latter age estimate is the result of a study that was based on the application of absolute dating methods on materials from Site 30, one of the largest smelting sites in the valley. Even more than providing absolute dates for the activities at Site 30, this study demonstrated the importance of the application of absolute dating methods to the sites in Timna, as typological, technological and other considerations are often confusing in this peripheral region (cf., Ben-Yosef *et al.* 2010a).

*Received 18 August 2016; accepted 22 February 2017
†Corresponding author: email ebenyose@post.tau.ac.il

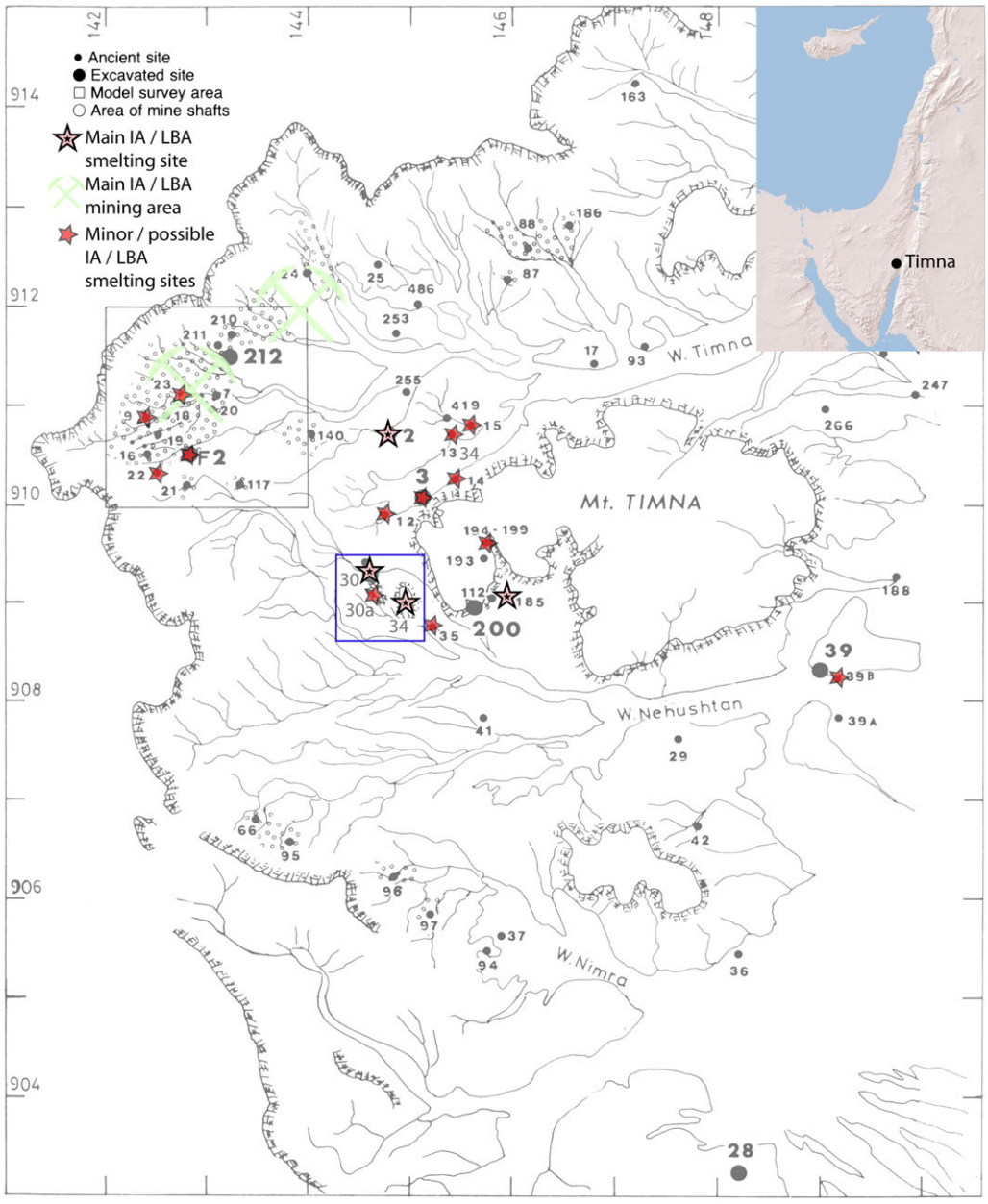

Figure 1 *The main copper production sites in the Timna Valley (after Rothenberg 1990). The research area is indicated with a blue square. [Colour figure can be viewed at wileyonlinelibrary.com]*

The current study is focused on Site 34 (‘Slaves’ Hill’/‘Khirbat Mene’iyah’), which is another of the main smelting camps in Timna, and on the smaller smelting camp of Site 30a (note that in this context, ‘site’ is used in the archaeological sense, as opposed to the common use in palaeomagnetism). Both sites are located in the centre of the valley and in close proximity to Site 30 (Fig. 1). The aim of the current study is to provide archaeomagnetic age constraints for

individual slag mounds within these sites, in order to better understand the history of copper production and its associated social organization.

In 2012, we conducted a survey of slag mounds at Site 34 and its surroundings (Figs 2–4), and at the nearby Site 30a (Figs 4 and 5). Together with Site 30, these sites represent the largest remains of copper smelting in Timna, with slag deposits located on hilltops (Sites 34 and 30a), inside a fortified encampment (Site 30) and in the open valley (slag mounds at the hill bottom of Site 34). Furthermore, it was noted that slag mounds on Site 34's hilltop are accompanied by stone-built installations, whereas those at the bottom of the hill are not.

In order to better understand the temporal context of the slag mounds, we collected slag samples from different mounds at Sites 34 (hilltop and hill bottom) and 30a (Fig. 4) for an archaeomagnetic investigation. The latter is located on a sandstone cliff above the large smelting camp of Site 30 and is difficult to access today (Fig. 5; it is possible that its original access path has collapsed since the site was abandoned), making the archaeomagnetic sampling one of the more feasible approaches for dating this site, as excavations would be logistically challenging. Here, we compare the archaeomagnetic intensity results from Sites 30a and 34 among themselves and with data from the previously dated Site 30 (Shaar *et al.* 2011), in order to glean temporal insights such as contemporaneity or lack thereof. In addition, we compare our new data with the changes in geomagnetic intensity in the Levant (Shaar *et al.* 2016). It should be noted that it is difficult to apply relative dating by ceramic typology in this area (cf., Ben-Yosef *et al.* 2010a), as sites in the Timna Valley are far from the core of the settled regions, where this typology was established, and the pottery assemblages are usually poor (hence the fluidity in dating mentioned above). Recently, sites in the Timna Valley have been successfully chronologically constrained by archaeomagnetic studies without relying on the highly debated ceramic typology of this area (Ben-Yosef *et al.* 2008a, 2010a, 2012). The research presented here

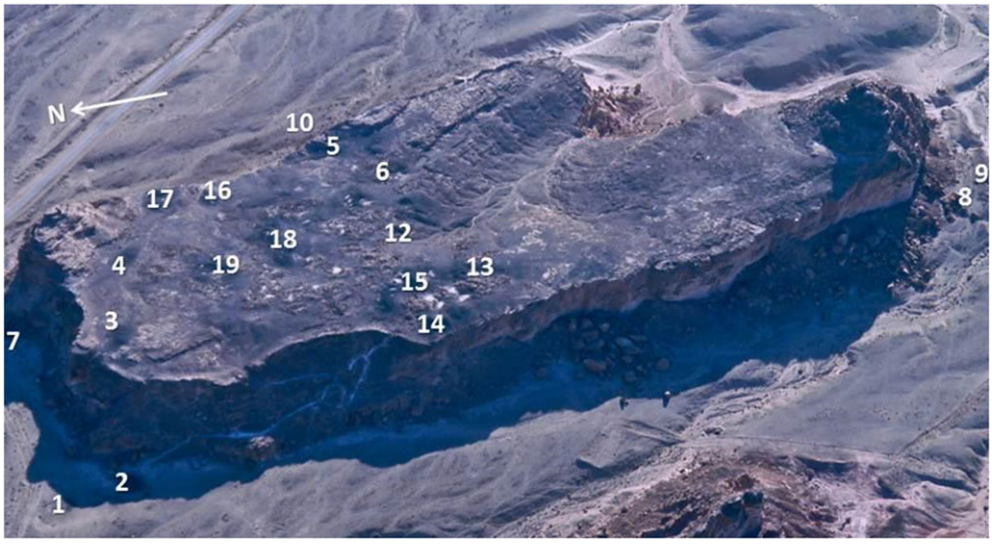

Figure 2 *An aerial view of Site 34 (the elongated hilltop is ~320 m long), with slag mounds numbered 1–19 after the 2012 survey undertaken as part of the current research (photograph courtesy of U. Avner). Slag Mounds 1 and 2 are referred to as coming from the 'base' of the hill (hill bottom), Slag Mounds 7 and 10 are on the hill slopes, and are likely to have slumped from higher up, while the rest are referred to as the 'hilltop' mounds. [Colour figure can be viewed at wileyonlinelibrary.com]*

Figure 3 *Slag Mound 17 recorded in the 2012 survey of Site 34 ('Slaves' Hill'). [Colour figure can be viewed at wileyonlinelibrary.com]*

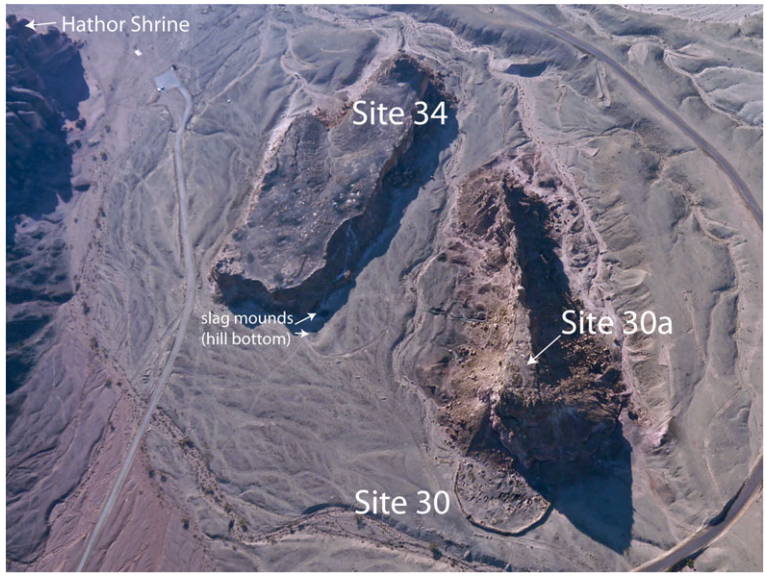

Figure 4 *An aerial photograph of the sites mentioned in the text (courtesy of U. Avner). [Colour figure can be viewed at wileyonlinelibrary.com]*

follows those studies, and focuses on direct archaeomagnetic investigation of slag, the waste by-product of the copper smelting process itself, thus limiting possible contextual biases.

Visible changes to the slag's appearance—that is, slag typology—can, in principle, be used as a *terminus post quem* dating reference to constrain the period in which the slag was created. For

Figure 5 *The sheer cliffs surrounding Site 30a. The archaeointensity results of this study demonstrate that copper smelting took place here during the early Iron Age. [Colour figure can be viewed at wileyonlinelibrary.com]*

example, a more advanced copper smelting technique was introduced to the region following Pharaoh Shoshenq I′s campaign during the second half of the 10th century BCE, which is reflected in the slag's visible size differences (Shaar *et al.* 2011; Ben-Yosef *et al.* 2012; Ben-Yosef and Levy 2014). Such information can be used to further narrow down the age constraints produced by archaeomagnetic data (below).

For the purpose of archaeomagnetic study, each piece of slag collected during the field survey was termed a 'sample'. Each sample was broken into several (between five and nine) 1–3 mm chips, termed 'specimens', which were subjected to the archaeointensity experiments. Each specimen was labelled with six characters: two letters representing the project name (tp = Timna Project), two digits representing the slag mound number as recorded by the 2012 survey, one letter representing the sample and one digit representing the specimen. For example, Sample tp01a1 is Specimen '1' of Sample 'a' from Slag Mound 01 of the current project.

MATERIALS AND METHODS

This study is aimed at providing age constraints on smelting activities at Sites 34 and 30a, based on changes in the intensity of the Earth's magnetic field ('secular variation'). The geomagnetic field fluctuates rapidly over centuries as a result of the complicated mechanism of its generation. It is represented by three geomagnetic attributes, (1) inclination, (2) declination and (3) intensity, which together produce a vector representation of the geomagnetic field specific to a time and place (Sternberg 1997). The current study is concentrated solely on intensity. Since the other attributes are directional, it is only possible to measure them if the object has not moved since its last heating event; for example, an intact smelting furnace (a rare find even in excavated

contexts in Timna). Because none of the material could be collected *in situ*, we focus here on the intensity recorded by the samples.

Background to archaeointensity experiments

Archaeological material acquires its remanent magnetization as follows. As a heated object cools, certain minerals in the object become magnetic and acquire a thermal remanent magnetization (TRM), which reflects the applied field (Tauxe 2010). When the magnetization of the specimen is analysed, the geomagnetic field at the time of the object's cooling can be determined in the laboratory and then compared to a known curve of regional changes, thus chronologically constraining the object to a limited period of time. Application of the so-called 'Thellier–Thellier based experiments' (a palaeointensity reconstruction based on gradual thermal demagnetisation; Thellier and Thellier 1959) on slag material has previously been studied by Ben-Yosef *et al.* (2008b) and Shaar *et al.* (2010), and here we follow similar experimental procedures.

In the current study we used the *IZZI* experimental protocol of Tauxe and Staudigel (2004), in which a specimen is heated to a specified temperature and cooled in a known magnetic field (in-field cooling), then reheated to the same temperature and cooled in a magnetic field of zero (zero-field cooling) which is the *IZ* step. The order of heating steps is then reversed such that the first heating/cooling step is done at a higher temperature and cooled in zero field followed by heating/cooling in the known field (the *ZI* step). The *IZ* and *ZI* steps alternate at increasingly higher temperatures until the sample is completely remagnetized and none of the original remanence remains. Included in the *IZZI* protocol are several tests applied to determine sample quality, namely the so-called partial thermal remanent magnetization (pTRM) check, whereby the specimen is reheated at a lower-temperature step and the pTRM gained in this second heating is compared to the original. A pTRM check is conducted in order to assess whether the specimen's capacity to acquire NRM has changed during the experiment.

The alternation between *IZ* and *ZI* steps itself constitutes a check on whether pTRMs acquired at a given temperature are entirely removed by reheating and cooling in zero field. If not, the remaining 'pTRM tails' create a zig-zag in the remanence remaining versus pTRM gained plots (so-called 'Arai plots'), a behaviour linked to non-ideal recording.

Cooling rates may also affect our ability to reconstruct the sample's ancient NRM, as slower cooling often results in a larger thermal remnant magnetization (Fox and Aitken 1980). However, slag cooled quickly in ancient times, and we can disregard the cooling rate effect.

Some archaeomagnetic samples acquire a TRM that is not exactly parallel to the applied field. They are anisotropic. Anisotropy, although typically quite minor in slag deposits (Ben-Yosef *et al.* 2008b), can be detected and corrected for, as the laboratory applied field is unlikely to be in the same direction with respect to the sample as the original cooling field. Therefore, we determined the anisotropy tensor by heating the specimens and cooling in six different orientations to the laboratory field. The specimens are heated to the highest temperature that had been used when determining the sample's NRM, with a seventh reheating of the specimens in the same position as the first heating in order to check whether the specimens' ability to acquire NRM has altered. In this experiment, we used a temperature of 580 °C and a magnetic field strength of 40 μT during anisotropy measurements. A total of 13 out of 44 successful specimens were tested for anisotropy. As the vast majority had a correction of less than 5%, we can assume that the average correction is similarly small.

RESULTS

The experimental data for this project were analysed via a Python package described by Tauxe *et al.* (2016), including Thellier GUI (Shaar and Tauxe 2013). Examples of the behaviour during the palaeointensity experiment are shown in Figure 6.

There are some 40 statistics that have been used at various times to screen out unreliable palaeointensity results (Paterson *et al.* 2014). Of these statistics, a typical study will use a subset that test for such problems as alteration, consistency and/or non-linearity of the results. Here, we use the statistics and threshold values listed in Table 1 for selection of specimen data. Statistics from all the successful specimens are listed in Table 2.

Multiple specimens that come from a single sample of slag are expected to have the same intensity within some error bounds, here taken to be within 10 μT or 15%. Results from samples

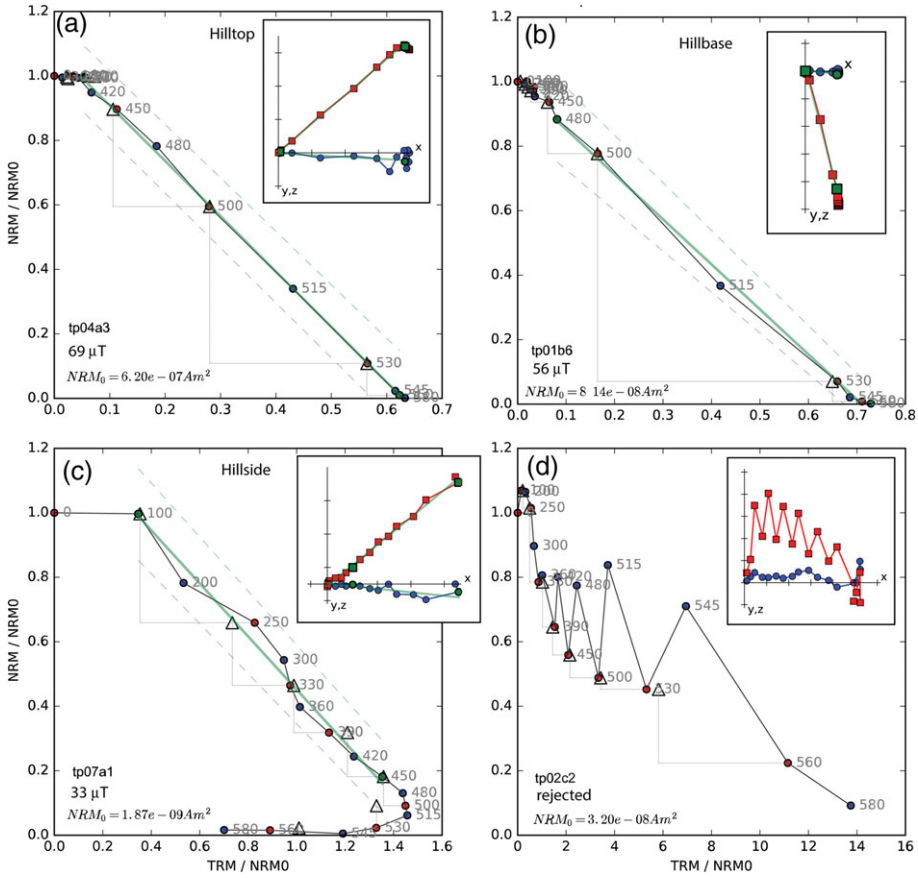

Figure 6 *Examples of 'Arai plots' from typical specimens, in which remaining remanence magnetizations are plotted against the partial thermal remanence gained at each temperature step (Tauxe 2010). The ZI (IZ) steps are shown as red (blue) dots, while pTRM check steps are shown as triangles. The slope of the best-fit line through the data points (shown in green) is used to calculate the intensity. The zero field steps plotted as vector components (X,Y as blue dots, X,Z as red squares) are shown in the insets. (a) Data for Specimen tp04a3 from Slag Mound 4 of Timna 34 hilltop. (b) Data for Specimen tp01b6 from Slag Mound 1 of Timna 34 (base). (c) Specimen tp07a1 from Timna 34 (hillside). (d) Specimen tp02c2 is an example of a rejected specimen. [Colour figure can be viewed at wileyonlinelibrary.com]*

Table 1 *The criteria used for the selection of palaeointensity specimens in this project*

Criteria abbreviation	*Criteria used*	*Definition*	*Failure in this criteria indicates*	*Source*
int_*n*	4	Minimum number of data points to be used from the chosen segment of the Arai plot	Not enough data for robust calculation	
int_ptrm_*n*	2	Minimum number of pTRM checks to be used from the chosen segment of the Arai plot	Specimen's ability to acquire NRM altered during the experiment	
FRAC	0.70	Fraction of the remanence	The data points in the chosen section represent a small fraction of the original remanence owing to multi-component behaviour or alteration during the experiment	Shaar and Tauxe (2013)
SCAT	TRUE	Scatter statistic meant to replace DRATS, Z and MD	The data points in the chosen section in the Arai plot are too scattered: the specimen has multi-domain magnetic grains or has suffered from alteration	Shaar and Tauxe (2013)
β	0.10	Scatter of data points about the best-fit line	Data affected by pTRM tails, or alteration	Shaar and Tauxe (2013)
MAD	6.5	Maximum angular deviation	Excessive scatter of Zijderveld plot due, for example, to zig-zagging from pTRM tails	Kirschvink (1980)
DANG	10.0	Deviation of ANGle	Deviation of the best-fit line in the Zijderveld plot caused by specimen carrying multi-component magnetization	Tauxe and Staudigel (2004)

meeting this test were converted to virtual axial dipole moments (VADMs; Tauxe 2010) which are listed, along with their 1σ uncertainties, in Table 3.

After determining which samples have reliable archaeointensity values, they are then compared to a regional master curve. A master curve shows what the expected intensity of the ancient geomagnetic field is for a given time and place within a restricted geographical distance of 1250–1500 km (Sternberg 1997; Valet 2003; Pavon-Carrasco *et al.* 2011). These master curves are based on archaeological samples the dates and archaeointensities of which are known. The master Levantine Archaeointensity Curve (LAC) used in this project is based on Shaar *et al.* (2016 and references therein).

During this project, 132 specimens from 34 samples were tested from the following 14 contexts: Slag Mounds 1 and 2 from Site 30a, and Slag Mounds 1, 2, 3, 4, 5, 6, 7, 10, 12, 13, 14 and 17 from Site 34. A total of 44 of the 132 specimens tested passed the specimen level criteria (Table 2), which gives a success rate of 33%. Demanding that at least two specimens per sample met the specimen-level criteria (which are quite strict) yielded a total of 17 samples. Of these, 13 samples had specimens that agreed with each other within 10 μT (~20 ZAm^2 for VADMs) or 15% for a success rate of 38% (Table 3). The rather low success rate on both sample and specimen levels is in accordance with previous studies on slag materials (cf., Ben-Yosef

Table 2 *The specimens and their archaeomagnetic results from this project: all specimens had a SCAT value of 'True'*

Specimen	*Int* (μT)	*DANG*	*FRAC*	*MAD*	*β*
tp01a2	53.3	6.06	0.75	6.43	0.04
tp01a4	53.29	1.69	0.72	2.46	0.04
tp01a6	53.13	2.23	0.92	5.46	0.03
tp01b1	57.92	0.44	0.91	4.96	0.02
tp01b3	43.95	3.04	0.72	6.46	0.07
tp01b6	55.84	1.43	0.76	1.03	0.03
tp01c1	61.64	0.5	0.76	3.1	0.02
tp01c3	59.46	0.24	0.81	2.01	0.01
tp01c4	52.78	0.22	0.79	3.61	0.04
tp02a2	60.48	0.68	0.88	6.24	0.02
tp02a3	51.61	0.99	0.72	2.82	0.02
tp03a1	40.9	9.49	0.93	4.49	0.04
tp03b1	104	0.3	0.77	6.37	0.03
tp04a1	80.31	5.28	0.77	6.32	0.04
tp04a2	58.69	0.11	0.91	6.06	0.03
tp04a3	68.62	0.37	0.77	4.56	0.01
tp04a4	62.09	0.13	0.91	1.81	0.01
tp04a5	73.45	0.75	0.7	3.64	0.03
tp04b2	62.91	2.02	0.75	4.46	0.01
tp04b3	62.88	5.11	0.72	4.45	0.04
tp04b4	63.04	3.2	0.72	4.96	0.04
tp04c4	72.7	0.4	0.76	6.17	0.03
tp05a2	68.11	0.2	0.89	2.59	0.03
tp05a3	74.53	1.02	0.85	3.87	0.03
tp06b3	53	4.86	0.87	6.08	0.03
tp07a1	32.94	1.09	0.74	5.56	0.06
tp07a3	39.06	2.88	0.7	5.26	0.1
tp10a4	76.6	0.62	0.74	6.38	0.04
tp10a5	53	1.01	0.98	2.97	0.03
tp10b1	41.9	0.7	0.89	3.85	0.03
tp12a2	65.01	1.68	0.71	2.17	0.01
tp12a3	55.33	0.15	0.95	2.73	0.02
tp12b2	58.57	0.22	0.7	2.11	0.01
tp12b3	62.83	0.75	0.72	6.1	0.06
tp13b1	55.12	1.57	0.73	5.68	0.05
tp13b2	63.88	2.03	0.74	3.08	0.06
tp14a3	52.3	0.76	0.91	4.08	0.03
tp14b1	64.7	0.33	0.98	2.01	0.02
tp17a1	66.51	1.72	0.82	5.8	0.03
tp17a2	66.54	1.92	0.74	4.77	0.05
tp17b3	85.2	1.25	0.7	3.48	0.05
tp21a2	67	0.94	0.99	5.02	0.03
tp22a3	65.83	0.75	0.71	2.41	0.06
tp22a4	75.43	1.04	0.77	5.46	0.05

et al. 2008b; Shaar *et al.* 2015, and see discussions therein); however, it should be noted that low success rates are common in archaeointensity experiments without clear correlation to material type (Valet 2003). In total, 9 of 14 contexts had multiple specimens from at least one sample that passed all criteria—a success rate of 64%—and we were therefore able to chronologically

Table 3 *Contexts that passed all criteria and their palaeomagnetic results as VADM (ZAm^2)*

Context (SM = Slag Mound)	*Sample*	*Number of specimens*	*VADM (ZAm^2)*	*VADM σ (ZAm^2)*	*σ (%)*
Timna 34, SM 1 (hill bottom)	tp01a	3	103.4	0.2	0.2
Timna 34, SM 1 (hill bottom)	tp01b	3	102.1	14.6	14.3
Timna 34, SM 1 (hill bottom)	tp01c	3	112.6	9.0	8.0
Timna 34, SM 2 (hill bottom)	tp02a	2	108.8	12.2	11.2
Timna 34, SM 4 (hilltop)	tp04a	5	133.3	16.9	12.7
Timna 34, SM 4 (hilltop)	tp04b	3	122.2	0.2	0.1
Timna 34, SM 5 (hilltop)	tp05a	2	138.5	8.8	6.4
Timna 34, SM 7 (hill slope)	tp07a	2	69.9	8.4	12.0
Timna 34, SM 12 (hilltop)	tp12a	2	116.9	13.3	11.4
Timna 34, SM 12 (hilltop)	tp12b	2	117.9	5.8	5.0
Timna 34, SM 13 (hilltop)	tp13b	2	115.6	12.0	10.4
Timna 34, SM 17 (hilltop)	tp17a	2	129.2	0.0	0.0
Timna 30a, SM 1 (hilltop)	tp22a	2	137.2	13.2	9.6

constrain a large number of slag mounds (see Table 3). The entire experimental data set and the results for all of the specimens will be uploaded into the MagIC online database (https://earthref.org/MAGIC/) upon publication.

The VADMs for the successful samples are plotted against well-dated Levantine data in Figure 7. Histograms of the data separated into hilltop and hill bottom (including the hill slope) are shown in Figure 8.

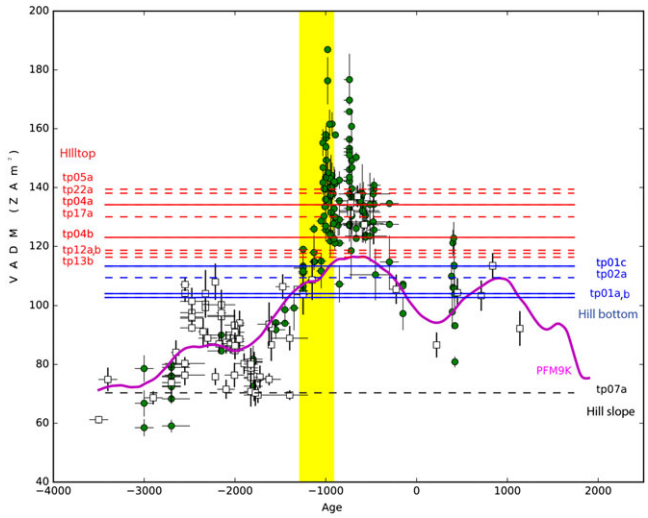

Figure 7 *Archaeomagnetic intensity results from slag mounds at Timna (this study) compared to data from the Levant (after Shaar et al. 2016 and references therein: filled green circles are data from the southern Levant and Cyprus; empty grey squares are data from northern Levant; the magenta line is the variations in VADM predicted by the PFM9K model of Nilsson et al. 2014). Dashed (solid) lines are for samples with N = 2 (> 2) specimens. The shaded area represents the main phase of copper production in Timna (13th to ninth centuries BCE). [Colour figure can be viewed at wileyonlinelibrary.com]*

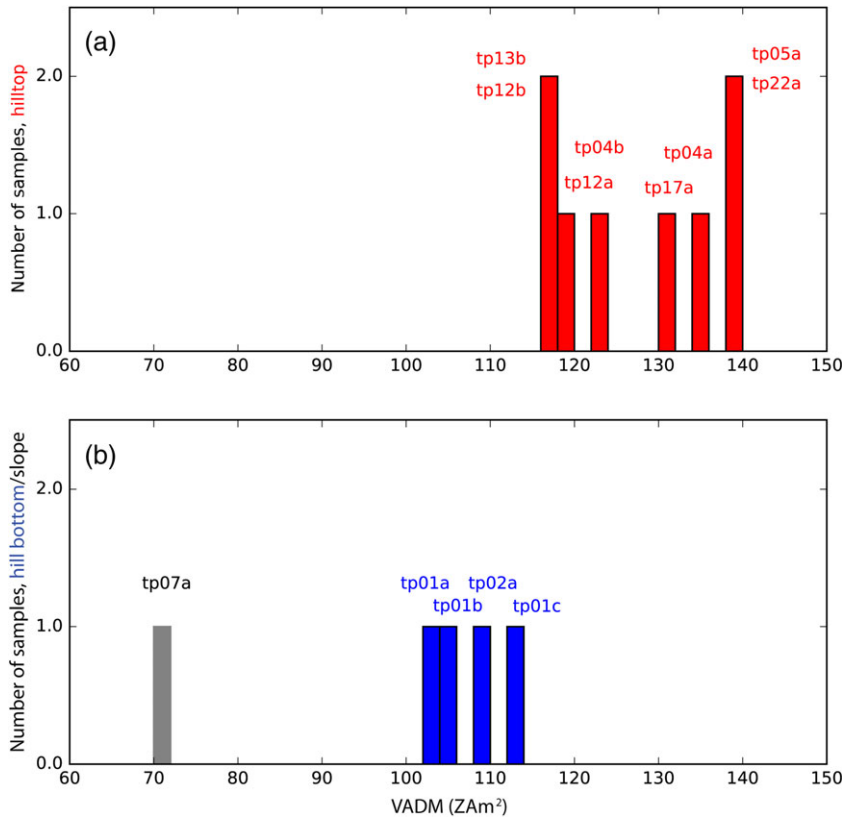

Figure 8 *Histograms of VADM values from samples collected from the hilltop slag mounds (red, upper plot) and those from the hill bottom and hill slope (blue and grey respectively, lower plot). [Colour figure can be viewed at wileyonlinelibrary.com]*

DISCUSSION

In general, results from hilltop sites have higher intensities than those from the hill bottom and the hill slope (Fig. 8). Moreover, these hilltop results are consistent with high values typical of the early Iron Age part of the Levantine Archaeomagnetic Curve (red lines in Fig. 7), whereas those from the base (including hill slope Slag Mound 7) are lower, consistent with either older ages or younger ages than the Iron Age high in the curve (blue lines in Fig. 7). Here follows is a more detailed analysis of the results.

Hilltop slag mounds: early Iron Age smelting

Site 30a. The archaeointensity values from Site 30a (Sample tp22a from Slag Mound 1; 29.4613°N, 34.5652°E) fit well with the early Iron Age (Fig. 7). Further refining of this slag mound's age is based on slag typology (Fig. 9). As previously mentioned, there are visible changes in the slag with varying technologies. The slag typology ('Type B' of Shaar *et al.* 2011) suggests that it is earlier than the second half of the 10th century BCE, when a new technology and slag type ('Type A', ibid.) were introduced to the region; however, the use of technological typologies as *terminus ante quem* should be done cautiously, and this suggestion is only tentative. No

Figure 9 *Slag at Timna 30a sampled in this study (note also the ground stones, used for crushing/grinding ore and slag, brought to the site from the valley below). [Colour figure can be viewed at wileyonlinelibrary.com]*

further refinements for dating Slag Mound 1 from Site 30a can be deduced from the intensity of the geomagnetic field in the Levant during the early Iron Age (Fig. 7); thus we conclude that it was created some time during the late 11th and 10th centuries BCE.

Site 34, Slag Mound 3. This slag mound is located at the north end of Site 34's hilltop (Fig. 2, 29.4612°N, 34.5703°E). Only two specimens from this mound passed our selection criteria (Table 2), but agreement between the two was quite poor, so definitive interpretation is not possible at this time. That said, one of the specimens has an extremely high intensity, consistent with the 'Iron Age Geomagnetic Spikes' documented recently by Ben-Yosef *et al.* (2009), Shaar *et al.* (2011) and Shaar *et al.* (2016) (Fig. 8). As copper production in Timna ceased for several centuries by the end of the ninth century BCE (Ben-Yosef *et al.* 2012), the high value from Slag Mound 3 only fits the earlier 'spike', which occurred between 990 and 970 BCE (Shaar *et al.* 2016; also cf., Shaar *et al.* 2011). Thus, we are able to tentatively date the smelting activity represented by this slag deposit to 980 ± 10 BCE, a dating resolution that is unprecedented even by other techniques such as radiocarbon.

Site 34, Slag Mound 4. This slag mound, which is also located in the northern area of Site 34's hilltop (29.4612°N, 34.5705°E), shows archaeomagnetic results that fit the Iron Age (tp04a, Fig. 7 and Table 3); we can tentatively suggest an early Iron Age date (11th–10th centuries BCE), based on our current knowledge that production in Timna ceased (for several centuries) in the late ninth century BCE, and slag typology ('Type B' of Shaar *et al.* 2011, and see above).

Site 34, Slag Mound 5. This slag mound is located at the western edge of Site 34's hilltop (29.4608°N, 34.5706°E), and also shows archaeomagnetic results that fit the Iron Age (tp05a, Fig. 7). Based on the same considerations outlined for Slag Mound 4 above, we can suggest an early Iron Age date (11th–10th centuries BCE).

Site 34, Slag Mound 12. This slag mound is located at the centre of the hilltop (29.4608°N, 34.5704°E). The archaeomagnetic results are among the lowest of the hilltop slag mounds

(Fig. 7), but are still higher than all the results from the hill bottom (Figs 7 and 8), and the value is consistent with those seen during the Iron Age (tp12a and tp12b, Fig. 7), the same period as other hilltop slag mounds.

Site 34, Slag Mound 13. This slag mound is located near the eastern edge of Site 34's hilltop (29.4607°N, 34.5703°E), and has comparable intensity to those of Slag Mound 12, suggesting that it is also dated to the Iron Age (tp13b, Fig. 7).

Site 34, Slag Mound 17. Archaeomagnetic results from Slag Mound 17, located in the northern part of the western edge of Site 34's hilltop (29.4610°N, 34.5705°E), have high results similar to those from Slag Mounds 4 and 5 from Site 34, and similarly should be dated to the Iron Age (tp17a, Fig. 7).

Hill bottom slag mounds: Early Islamic smelting?

Site 34, Slag Mound 1. The archaeomagnetic results from Sample tp01a from Site 34's Slag Mound 1, located at the bottom of the hill (29.4613°N, 34.5701°E), rule out the Iron Age, and instead are consistent with the Late Bronze Age, the Roman period or the Early Islamic period (Fig. 7). Slag typology indicates an advanced tapping technology, which is not known in the Arabah prior to the late 10th century BCE (Ben-Yosef and Levy 2014); together with distinct wrinkles (Fig. 10) and a diagnostic pottery sherd found nearby, the most reasonable date for this mound is the Early Islamic period (*c*.640–1000 CE). The results of Sample tp01b from Site 34's Slag Mound 1 are statistically identical to those for tp01a (Table 3 and Fig. 7), and those of Sample tp01c are slightly higher, but still fit with the Islamic period. The latter might suggest that smelting activities at this location represent a relatively long time span within the Early Islamic period (at least of a few generations), rather than an ephemeral smelting episode.

Figure 10 *Slag fragments at Slag Mound 2, Site 34, Timna; wrinkles may be indicative of Early Islamic smelting technology. [Colour figure can be viewed at wileyonlinelibrary.com]*

Site 34, Slag Mound 2. The archaeomagnetic results from Sample tp02a from Site 34's Slag Mound 2, located at the bottom of the hill (29.4612°N, 34.5701°E) are similar to those of Slag Mound 1, although slightly higher than Samples tp01a and tp01b (Fig. 7). Here also, the same considerations mentioned in discussing Slag Mound 1 suggest the Early Islamic period as the time of its creation.

Slag Mound 7: Early Bronze Age smelting?

Slag Mound 7 is a scatter of small fragments of greyish slag, located on the northern lower slope of Site 34's hill (Fig. 2, 29.7702°N, 34.9515°E). The archaeointensity value retrieved for this mound is the lowest of all slag mounds investigated in this study and fits best to the Early and Middle Bronze Ages (Figs 7 and 8). While there is no evidence of copper production in Timna and the Arabah Valley during the Middle Bronze Age (*c.*1950–1550 BCE), in the Early Bronze Age (EBA) the copper industry in the region flourished (Hauptmann 2007; Ben-Yosef *et al.* 2016). The evidence for EBA production comes mostly from Faynan copper ore district and the northern Arabah, where dozens of sites indicate intense activity during the EBA II–III transition (around 2900 BCE) and the late EBA III – EBA IV periods (*c.*2600–1950 BCE). Within the EBA, the archaeointensity value of Slag Mound 7 fits best the EBA II–III transition, and is statistically identical to recently published values retrieved from slag of this period from Khirbat Hamra Ifdan in Faynann (69.9 ± 8.4 versus 68 ± 1 ZAm^2 VADM, respectively; see Ben-Yosef *et al.* 2016).

Throughout the third millennium BCE, copper smelting was conducted by wind-blown furnaces located on hilltops at Faynan and the Arabah (Genz and Hauptmann 2002; Hauptmann 2007). It is therefore reasonable to assume that Slag Mound 7 represents EBA II–III copper smelting activities, which were conducted by wind-blown furnaces on the edge of the hilltop (where they were typically located). In fact, the spill and/or collapse of slag material on to the slope enabled the preservation of this unique evidence, as the hilltop was extensively used for copper smelting during the Iron Age (as demonstrated by the current study). Moreover, it is likely that EBA slag on the hilltop were reused during the Iron Age smelting activities, thus completely erasing evidence of the earlier phase (cf., Hauptmann 2007).

CONCLUSIONS

The results of the current study add to previous research on slag as a palaeomagnetic recorder (Ben-Yosef *et al.* 2008b; Shaar *et al.* 2010, 2015) and further demonstrates the potential of archaeomagnetic studies to provide age constraints on industrial contexts in archaeological research. This archaeointensity experiment yielded insights on the dating of slag, the most common find at metal smelting sites. Sites with slag mounds in the Timna Valley as well as copper smelting sites around the world can be chronologically constrained using this method according to the procedures and caveats as detailed above. The method has several advantages, among them the direct dating of artefacts (in cases where these artefacts are the *objective* of the study) without relying solely on contextual considerations, and with no need for excavations to clarify contexts (the current work was based on a two-day survey of slag mounds).

During this project, we achieved a success rate of 33% at the specimen level, and a 38% success rate at the sample level. The successful samples allowed 9 of the 14 sampled contexts to be age constrained to various periods—Slag Mound 1 from Site 30a and Slag Mounds 4, 5,

12, 13 and 17 from Site 34 to the early Iron Age, Slag Mounds 1 and 2 from Site 34 to the Early Islamic period, and Slag Mound 7 to the Early Bronze Age—a success rate of 64%.

All slag mounds located on hilltops, both Site 34's hilltop and Site 30a, were constrained to the early Iron Age. The date of the former has been supported by recent excavations at Site 34 and new radiocarbon dates (although not from the same slag mounds; Ben-Yosef 2016). As the hilltops are naturally protected by cliffs, a need for security during this period is implied. It is important to note that at this technological stage, wind was not used to aerate the furnaces (Rothenberg 1990; Hauptmann 2007). Another emphasis, on defence, is reflected in the walls built around Site 34's hilltop and the Iron Age smelting camp of Site 30 (Rothenberg 1980; Ben-Yosef 2016). This is consistent with our knowledge of the society operating the Arabah copper mines during this period (Levy *et al.* 2014), which was engaged in military conflicts with nearby polities, in a time when local kingdoms such as ancient Israel and Edom emerged in the southern Levant (Ben-Yosef *et al.* 2010b). On the other hand, the slag deposits of the Early Islamic period are located in the valley, in open, unprotected contexts, and reflect a time of stability when the region was deep within the territory of the Islamic empires (the Umayyad and/or the Abbasid, *c*.640–1000 CE). While the Early Islamic activities seem to be relatively limited in the centre of the Timna Valley, the early Iron Age slag mounds are large and numerous, indicating intense copper smelting during the 11th–10th centuries BCE. This phase of extensive production in the Timna Valley is contemporaneous to the main phase of copper smelting in Faynan, the other substantial copper ore district within the Arabah Valley (and the largest; Levy *et al.* 2014).

In addition to the two periods mentioned above, our study provides evidence of an earlier phase of copper smelting done on the hilltop of Site 34 and dated to the EBA II–III. Although there is abundant evidence for copper production in this period in Faynan and the northern Arabah, there are only a few EBA II–III sites in the southern Arabah and until now none from the Timna Valley itself. Thus, the new results add a significant contribution to our understanding of early third millennium BCE exploitation of the Timna copper ore.

In conclusion, the age constraints provided by this study on various slag mounds enabled an assessment of the scale of production and differences in organization of production between distinct archaeological periods. In addition, the results demonstrate the potential of archaeomagnetic investigation to the dating of heated materials, especially when used in combination with contextual and typological data.

ACKNOWLEDGEMENTS

We thank Jason Steindorf and Yael Ebert for their help in preparing and measuring some of the samples used in this study, and Ron Shaar for his sage advice. This project was supported by the Marie Curie Career Integration Grant (CIG) #33427 to E.B.-Y., the United States – Israel Binational Science Foundation, Grant #20112359 to E.B.-Y. and L.T., and by the United States National Science Foundation grant #EAR1345003 to L.T.

REFERENCES

Ben-Yosef, E., 2016, Back to Solomon's era: results of the first excavations at Slaves' Hill (Site 34, Timna, Israel), *Bulletin of the American Schools of Oriental Research*, **376**, 169–98.

Ben-Yosef, E., and Levy, T. E., 2014, The material culture of Iron Age copper production in Faynan, in *New insights into the Iron Age archaeology of Edom, southern Jordan* (eds. T. E. Levy, M. Najjar, and E. Ben-Yosef), 887–959, Cotsen Institute of Archaeology, UCLA, Los Angeles, CA.

Ben-Yosef, E., Tauxe, L., and Levy, T. E., 2010a, Archaeomagnetic dating of copper smelting site F2 in the Timna Valley (Israel) and its implications for the modelling of ancient technological developments, *Archaeometry*, **52**, 1110–21.

Ben-Yosef, E., Shaar, R., Tauxe, L., and Ron, H., 2012, A new chronological framework for Iron Age copper production in Timna (Israel), *Bulletin of the American Schools of Oriental Research*, **367**, 31–71.

Ben-Yosef, E., Levy, T. E., Higham, T., Najjar, M., and Tauxe, L., 2010b, The beginning of Iron Age copper production in the southern Levant: new evidence from Khirbat al-Jariya, Faynan, Jordan, *Antiquity*, **84**(325), 724–46.

Ben-Yosef, E., Gidding, A., Tauxe, L., Davidovich, U., Najjar, M., and Levy, T. E., 2016, Early Bronze Age copper production systems in the northern Arabah Valley: new insights from archaeomagnetic study of slag deposits in Jordan and Israel, *Journal of Archaeological Science*, **72**, 71–84.

Ben-Yosef, E., Tauxe, L., Levy, T. E., Shaar, R., Ron, H., and Najjar, M., 2009, Geomagnetic intensity spike recorded in high resolution slag deposit in southern Jordan, *Earth and Planetary Science Letters*, **287**(3–4), 529–39.

Ben-Yosef, E., Tauxe, L., Ron, H., Agnon, A., Avner, U., Najjar, M., and Levy, T. E., 2008a, A new approach for geomagnetic archaeointensity research: insights on ancient metallurgy in the southern Levant, *Journal of Archaeological Science*, **35**, 2863–79.

Ben-Yosef, E., Ron, H., Tauxe, L., Agnon, A., Genevey, A., Levy, T. E., Avner, U., and Najjar, M., 2008b, Application of copper slag in geomagnetic archaeointensity research, *Journal of Geophysical Research*, **113**(B08101).

Conrad, H. G., and Rothenberg, B. (eds.), 1980, *Antikes Kupfer im Timna-Tal*, Der Anschnitt Beiheft 1, Bochum, Deutsches Bergbau-Museum.

Fox, J. M. W., and Aitken, M. J., 1980, Cooling-rate dependence of thermoremanent magnetization, *Nature*, **283**, 462–3.

Genz, H., and Hauptmann, A., 2002, Chalcolithic and EBA metallurgy in the southern Levant, in *Anatolian metal II* (ed. U. Yalcin), 149–58, Der Anschnitt Beiheft 15, Deutsches Bergbau-Museum, Bochum.

Glueck, N., 1935, Explorations in eastern Palestine, II, in *Annual of the American Schools of Oriental Research*, 19–288, American Schools of Oriental Research, New Haven, CT.

Hauptmann, A., 2007, *The archaeometallurgy of copper: evidence from Faynan*, Jordan, Berlin, Springer.

Kirschvink, J. L., 1980, The least-squares line and plane and the analysis of paleomagnetic data, *Geophysical Journal of the Royal Astronomical Society*, **62**, 699–718.

Levy, T. E., Najjar, M., and Ben-Yosef, E., 2014, *New insights into the Iron Age archaeology of Edom, southern Jordan*, Cotsen Institute of Archaeology, UCLA, Los Angeles, CA.

Nilsson, A., Holme, R., Korte, M., Suttie, N., and Hill, M., 2014, Reconstructing Holocene geomagnetic field variation: new methods, models and implications, *Geophysical Journal International*, **198**, 229–48.

Paterson, G. A., Tauxe, L., Biggin, A., Shaar, R., and Jonestrask, L., 2014, On improving the selection of Thellier-type paleointensity data, *Geochemistry, Geophysics, Geosystems*, **15**(4), 1180–92.

Pavon-Carrasco, F., Rodrigues-Gonzalez, J., Osete, M. L., and Torta, J. M., 2011, A MATLAB tool for archaeomagnetic dating, *Journal of Archaeological Science*, **38**(2), 408–19.

Rothenberg, B., 1980, Die Archaologie des Verhuttungslagers Site 30, in *Antikes Kupfer im Timna-Tal* (eds. H. G. Conrad and B. Rothenberg), 187–213, Deutsches Bergbau-Museum, Der Anschnitt Beiheft 1, Bochum.

Rothenberg, B. (ed.), 1990, *Researches in the Araba 1959–1984*, Vol. **2,** *The ancient metallurgy of copper*, Institute for Archaeo-Metallurgical Studies, London.

Rothenberg, B., 1999a, Archaeo-metallurgical researches in the southern Arabah 1959–1990. Part 1: Late Pottery Neolithic to Early Bronze IV, *Palestine Exploration Quarterly*, **131**, 68–89.

Rothenberg, B., 1999b, Archaeo-metallurgical researches in the southern Arabah 1959–1990. Part 2: Egyptian New Kingdom (Ramesside) to Early Islam, *Palestine Exploration Quarterly*, **131**, 149–75.

Rothenberg, B., and Glass, J., 1992, Beginnings and development of early metallurgy and the settlement and chronology of the western Arabah, from the Chalcolithic period to Early Bronze Age IV, *Levant*, **24**, 141–57.

Shaar, R., and Tauxe, L., 2013, Thellier GUI: an integrated tool for analyzing paleointensity data from Thellier-type experiments, *Geochemistry, Geophysics, Geosystems*, **14**, 677–92.

Shaar, R., Ben-Yosef, E., Ron, H., Tauxe, L., Agnon, A., and Kessel, R., 2011, Geomagnetic field intensity: How high can it get? How fast can it change? *Constraints from Iron Age copper-slag from the southern Levant, Earth and Planetary Science Letters*, **301**, 297–306.

Shaar, R., Ron, H., Tauxe, L., Kessel, R., Agnon, A., Ben-Yosef, E., and Feinberg, J. M., 2010, Testing the accuracy of absolute intensity estimates of ancient geomagnetic field using copper slag material, *Earth and Planetary Science Letters*, **290**(1–2), 201–13.

Shaar, R., Tauxe, L., Ben-Yosef, E., Kassianidou, V., Lorentzen, B., Feinberg, J. M., and Levy, T. E., 2015, Decadal-scale variations in geomagnetic field intensity from ancient Cypriot slag mounds, *Geochemistry, Geophysics, Geosystems*, **16**, 195–214.

Shaar, R., Tauxe, L., Ron, H., Ebert, Y., Zuckerman, S., Finkelstein, I., and Agnon, A., 2016, Large geomagnetic field anomalies revealed in Bronze and Iron Age archaeomagentic data from Tel Megiddo and Tel Hazor, *Israel, Earth and Planetary Science Letters*, **442**, 173–85.

Sternberg, R. S., 1997, Archaeomagnetic dating, in *Chronometric dating in archaeology* (eds. R. E. Taylor and M. J. Aitken), Plenum Press, New York.

Tauxe, L., 2010, *Essentials of paleomagnetism*, University of California Press, Berkeley, CA.

Tauxe, L., and Staudigel, H., 2004, Strength of the geomagnetic field in the Cretaceous Normal Superchron: new data from submarine basaltic glass of the Troodos Ophiolite, *Geochemistry, Geophysics, Geosystems*, **5**(2), Q02H06, https://doi.org/10.1029/2003GC000635.

Tauxe, L., Shaar, R., Jonestrask, L., Swanson-Hysell, N. L., Minnett, R., Koppers, A. A. P., Constable, C. G., Jarboe, N., Gaastra, K., and Fairchild, L., 2016, PmagPy: software package for paleomagnetic data analysis and a bridge to the Magnetics Information Consortium (MagIC) database, *Geochemistry, Geophysics, Geosystems*, **17**, 2450–63.

Thellier, E., and Thellier, O., 1959, Sur l'intensité du champ magnétique terrestre dans le passé historique et géologique, *Annales de Géophysique*, **15**, 285–378.

Valet, J.-P., 2003, Time variations in geomagnetic intensity, *Reviews of Geophysics*, **41**, https://doi.org/10.1029/2001RG000104.